

Study of microparticle incorporation in coating on titanium produced by plasma electrolytic oxidation (PEO)

F. Ceccarini, L. Calabrese, M.V. D'Alagni, M. Orefice, M. Pedefe

This research is focused on the analysis of the influence of rutile (TiO_2) and anatase (TiO_2) microparticles ($d < 5 \mu\text{m}$) on the morphology, structure, and anticorrosive properties of PEO coatings on titanium produced in alkaline based solution containing sodium hydroxide and sodium metasilicates or nanoclay particles (hydrophilic bentonite, $\text{H}_2\text{Al}_2\text{O}_6\text{Si}$, $d < 25 \mu\text{m}$).

PEO coatings are characterized by scanning electron microscope (SEM), energy dispersive spectroscopy (EDS) and X-ray diffraction (XRD). In addition, the samples are electrochemically investigated by electrochemical impedance spectroscopy analysis.

The tests carried out have shown that the incorporation of TiO_2 microparticles in the coating leads to the formation of thick oxide layers characterized by a fine porosity. These coatings provide good corrosion protection when samples are

INTRODUCTION

Plasma electrolytic oxidation (PEO) is a surface treatment that allows the formation of an oxide layer on titanium, aluminum, and magnesium. The process is immersed in an electrolyte solution and connected to a power source. The titanium (the anode) is connected to the positive terminal, while the cathode can allow the formation of an oxide layer. The oxide with microparticles. The ceramic coating is formed in the presence of the microparticles, which are incorporated by the aggregation of the particles. When the sample is exposed to a corrosive environment, the oxide layer causes a reduction in the corrosion rate. The treated components are subjected to various conditions through the electrochemical process. The electrochemical process is a self-limiting process that favors the formation of a dense oxide layer. The filling of the pores within the oxide layer is a key factor for the anticorrosive properties of the coating. The incorporation of microparticles in the coating is a promising technique for improving the anticorrosive properties of the coating.

F. Ceccarini, L. Calabrese, M.V. D'Alagni, M. Orefice, M. Pedefe

Dept. of Chemistry, Materials and Chemical Engineering "G. Natta",
Politecnico di Milano, Via Mancinelli 7, 20131 Milano, Italy

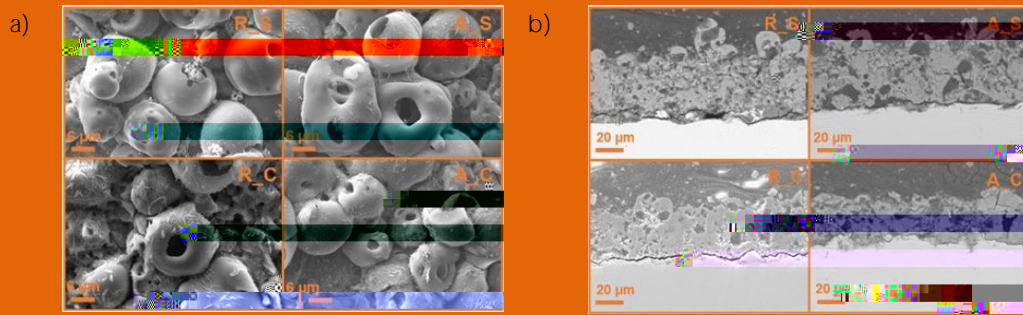
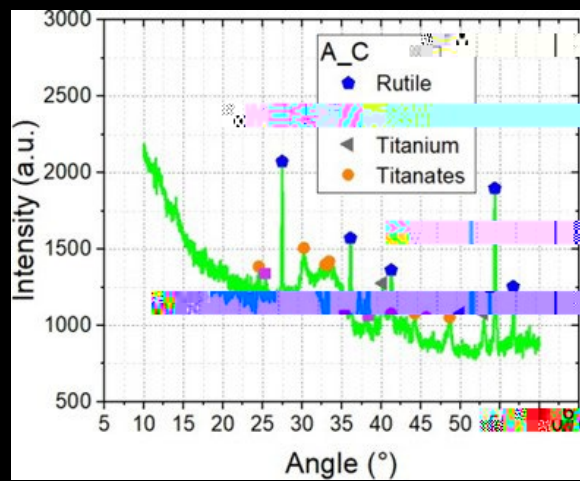


Fig. 1 - a) SEM images of the surfaces of PEO samples; b) SEM images of the cross-sections of PEO samples.

The analysis of the sections of the coatings using SEM (Fig. 1 b) allows to estimate the thickness of the oxides. By working with rutile particles, coatings with thicknesses of approximately 52 μm (R_S) and 35 μm (R_C) are reached, in the presence of silicates and nanoclay respectively. As regards the samples treated with anatase, thicknesses of approximately 49 μm (A_S) using silicates and 30 μm (A_C) in the presence of nanoclay are obtained.

It could be noted that the greater thicknesses are achieved by working with metasilicates in addition to the microparticles. This is the result of a double effect, i.e. the presence of silicates reduces the porosity of the coating, and its growth, and the presence of microparticles. Another important factor is the presence of the oxides, which leads to a decrease in porosity, and in electrolytic cells, the presence of porosity, the

microparticles are characterized by larger pores. These large defects may compromise the corrosion protection effect as they allow the penetration of the aggressive solution through the oxide. Coatings produced in the presence of rutile particles are instead characterized by the presence of cracks at the interface between the substrate and the oxide itself; this defect could potentially compromise the adhesion of the coating to the substrate. The EDS analyses (not reported) allow to verify the presence of Ti, O, Na and Si in all the samples. Furthermore, in the coatings



The XRD analysis is shown in Figure 2, in the presence of

Comparing the results of the impedance tests obtained from the PEO specimens with those of the untreated Ti grade 2 (Fig. 4. a), it is observed that the behavior of the samples changes significantly. The Nyquist diagram of bare Ti presents a double semicircle typical of a corrosive process and a polarization resistance, R_p (defined as the intersection of the arcs that interpolate the Nyquist graphs with the axis of the real impedance Z') typical of an active electrode (about $70 \Omega \text{ cm}^2$). [11] The specimens coated with PEO oxides, instead, show only one capacitive semicircle and R_p values that are four and five orders of magnitude higher for the samples treated with nanoclays and metasilicates, respectively, compared to Ti grade 2. These values demonstrate the corrosion protection ability of PEO coatings.

Looking in more detail at the graphs relating to PEO coatings (Fig. 3) it is immediately possible to notice an important difference between the oxides produced using the two different types of Si-containing additives.

First of all, the impedance curves of the samples treated with nanoclays present a significantly reduced diameter, an indication of a lower corrosion rate. The values of R_C and A_C values are similar to those obtained in the same conditions for the untreated section, but the diameter is approximately 10 times smaller. The samples prepared with metasilicates, instead, with larger diameters, are observed. The values of R_C and A_C indicated for the untreated sample Ti grade 2 can therefore be partly justified by the presence of the two types of Si-containing additives. R_S and A_S values are greater than those obtained for the nanoclay; this is due to the fact that by making the coating thicker, the consequent increase in the surface area by studying the diameter of the semicircle values it can be observed that the diameters decrease. Comparing the values of R_C and A_C and R_S and A_S indicates that the corrosion solution. The

of corrosion products that fill the pores of the coating, improving its corrosion protection effect.

Finally, it is noted that the impedance values achieved by A_S and A_C are slightly higher than those obtained by their respective rutile-containing counterparts. This phenomenon is probably due to the lower crystallinity of the samples produced through the incorporation of anatase particles, which therefore provide greater resistance to the passage of electrons generating higher impedances. However, it has been widely demonstrated that rutile guarantees better behavior against acid corrosion in long-term tests. [12]

By observing the trend of the imaginary impedance, it is possible to evaluate the kinetics of the ongoing relaxation phenomena. The diagrams obtained (not shown) present a single time constant at low frequencies therefore attributable to a corrosion reaction controlled by the diffusion of aggressive species through the coating. [13]

CONCLUSIONS

This paper describes the results of the electrochemical

BIBLIOGRAPHY

- [1] S. Sikdar, P. V. Menezes, R. Maccione, T. Jacob, and P. L. Menezes, "Plasma electrolytic oxidation (PEO) process—processing, properties, and applications," *Nanomaterials*, vol. 11, no. 6, 2021, doi: 10.3390/nano11061375.
- [2] X. Lu, C. Blawert, M. L. Zheludkevich, and K. U. Kainer, "Insights into plasma electrolytic oxidation treatment with particle addition," *Corros. Sci.*, vol. 101, pp. 201–207, 2015, doi: 10.1016/j.corsci.2015.09.016.
- [3] A. Fattah-alhosseini, M. Molaei, and K. Babaei, "The effects of nano- and micro-particles on properties of plasma electrolytic oxidation (PEO) coatings applied on titanium substrates: A review," *Surfaces and Interfaces*, vol. 21, no. December 2019, p. 100659, 2020, doi: 10.1016/j.surfin.2020.100659.
- [4] X. Lu et al., "Plasma electrolytic oxidation coatings with particle additions – A review," *Surf. Coatings Technol.*, vol. 307, pp. 1165–1182, 2016, doi: 10.1016/j.surfcoat.2016.08.055.
- [5] S. Moon and Y. Jeong, "Generation mechanism of microdischarges during plasma electrolytic oxidation of Al in aqueous solutions," *Corros. Sci.*, vol. 51, no. 7, pp. 1506–1510, 2009, doi: 10.1016/j.sa.9o5 0.1016mT u1016/j/j/j/.ST6c39.
- [6] X. Zhang et al., "X-ray Computed Tomographic Investigation of the Porosity and Morphology of Plasma Electrolytic Oxidation Coatings," *ACS Appl. Mater. Interfaces*, vol. 8, no. 13, pp. 8801–8810, 2016, doi: 10.1021/acsami.6b00274.
- [7] E. Matykina, A. Berkani, P. Skeldon, and G. E. Thompson, "Real-time imaging of coating growth during plasma electrolytic oxidation of titanium," *Electrochim. Acta*, vol. 53, no. 4, pp. 1987–1994, 2007, doi: 10.1016/j.electacta.2007.08.074.
- [8] D. A. H. Hanaor and C. C. Sorrell, "Review of the anatase to rutile phase transformation," *J. Mater. Sci.*, vol. 46, no. 4, pp. 855–874, 2011, doi: 10.1007/s10853-010-5113-0.
- [9] S. Aliasghari, P. Skeleton, and G. E. Thompson, "Plasma electrolytic oxidation of titanium in a phosphate/silicate electrolyte and tribological performance of the coatings," *Appl. Surf. Sci.*, vol. 316, no. 1, pp. 463–476, 2014, doi: 10.1016/j.tapsusc.2014.08.037.
- [10] X. Chen and S. S. Mao, "Titanium dioxide nanomaterials: Synthesis, properties, modifications and applications," *Chem. Rev.*, vol. 107, no. 7, pp. 2891–2959, 2007, doi: 10.1021/cr0500535.
- [11] L. Casanova, M. La Padula, M. P. Pedferri, M. V. Diamanti, and M. Ormellese, "An insight into the evolution of corrosion resistant coatings on titanium during bipolar plasma electrolytic oxidation in sulfuric acid," *Electrochim. Acta*, vol. 379, p. 138190, 2021, doi: 10.1016/j.electacta.2021.138190.
- [12] L. Casanova, M. Arosio, M. T. Hashemi, M. Pedferri, G. A. Botton, and M. Ormellese, "Influence of stoichiometry on the corrosion response of titanium oxide coatings produced by plasma electrolytic oxidation," *Corros. Sci.*, vol. 203, no. January, p. 110361, 2022, doi: 10.1016/j.corsci.2022.110361.
- [13] L. Casanova, F. Ceriani, M. Pedferri, and M. Ormellese, "Addition of Organic Acids during PEO of Titanium in Alkaline Solution," *Coatings*, vol. 12, no. 12, p. 2020143, 2022, doi: 10.3390/coatings12020143.

[TORNA ALL'INDICE >](#)